

Fine structure of the inner electric field in semiconductor laser diodes studied by EFM.

A.Ankudinov¹, V.Marushchak¹, A.Titkov¹, V.Evtikhiev¹, E.Kotelnikov¹, A.Egorov¹,
H.Riechert², H.Huhtinen³, R.Laiho³

¹ Ioffe PTI, Polytechnicheskaya 26, St.-Petersburg, 194021, Russia

² Infineon Technologies AG, Corporate Research, D-81730 München, Germany

³ Wihuri Physical Laboratory, Turku University, Turku, FIN20014, Finland

Email:Alexander.Ankudinov@pop.ioffe.rssi.ru; FAX 812-2471017

Abstract. Electrostatic force microscopy in dynamical contact and noncontact modes is employed to study the distribution of the electric field and capacitance at the cleavages of AlGaAs/GaAs based p-i-n laser diode heterostructures. The fine structure of the inner electric field located at the i-waveguide of the laser heterostructure is revealed and investigated under forward and backward biases applied to the diode. The redistribution of the electric field in favor of i-waveguide/p-emitter interface is observed at high level of injected current. When the injected current increase, the growth of the capacitance signal at the i-waveguide is also detected, that may reflect the injected carriers distribution.

The inner electric characteristics of the semiconductor devices under the conditions close to the operation are the subject of intensive theoretical and experimental interest. Very attractive possibilities on the high resolution mapping of the electric field and capacitance distribution in the semiconductor structures are provided by the relatively new method of electrostatic force microscopy (EFM)[1]. In the first studies [2,3,4] focused on the application of EFM to probe electric characteristics of semiconductor light emitting devices, the main attention was concentrated on the potential profiles across the devices, the capacitance distributions had a minor attention. Besides, the authors used noncontact mode electrostatic force microscopy (NC EFM), when the probe performs resonant oscillations at some distance from the surface. Recently the dynamic contact mode electrostatic force microscopy (DC EFM) was developed [5], in which the probe is in the constant contact with the studied surface. In this case the distance between the probe and the surface is minimized, what may provide better sensitivity and resolution of the EFM. Successful attempt to apply

the DC EFM for studying the semiconductors laser diodes is presented in our recent work [6].

In this work we have performed EFM studies in DC and NC modes to investigate the electric field and capacitance distributions on the cross-sections of the AlGaAs/GaAs based p-i-n laser diodes under the applied forward and backward biases. We show that on the atomically flat cleavages of laser heterostructures both modes demonstrate self consisting results. The electric field distribution in the studied laser structures has two field maximums localized at the n-emitter/i-waveguide and p-emitter/i-waveguide interfaces. At the low level of the injection current the inner electric field induced by the applied bias is concentrated mainly in the vicinity of the n-emitter/i-waveguide interface, while at the high level of injection it is redistributed in favor of the p-emitter/i-waveguide interface. With increasing forward bias the growth and broadening of the capacitance signal at the undoped waveguide region is also observed, that may reflect the injected carriers distribution.

Consider the main principles of the EFM [2-5]. If the conductive probe is at some potential U relative to the sample, then the acting electrostatic force can be written as:

$$F_{el}=1/2\times d(C_{ps}U^2)/dz \quad (1),$$

where C_{ps} is the capacitance between the probe and sample and an axe z is perpendicular to the sample surface. The potential U between the probe and sample surface may be written as $U=U_{dc}+U_{ac}\cos(\omega t)+V_{ps}$, where U_{dc} is external dc bias, $U_{ac}\cos(\omega t)$ is ac bias and V_{ps} is the contact potential between the probe and the sample. Substitution of this expression into formula (1) shows, that the resulting force F_{el} will have three components: one static and two alternating, oscillating at the frequencies ω and 2ω . The oscillating components are given by:

$$F(\omega)=(dC_{ps}/dz)(U_{dc}+V_{ps})U_{ac}\cos(\omega t) \quad (2),$$

$$F(2\omega)=1/4(dC_{ps}/dz)U_{ac}^2\cos(2\omega t) \quad (3).$$

In the EFM method the oscillating components of the electrostatic force induce mechanical oscillations of the AFM probe. The first and the second harmonics ($H(\omega)$, $H(2\omega)$) of oscillations, which are the two main EFM signals, can be detected by lock-in technique. $H(\omega)$ depends mainly on the probe-surface potential difference, $H(2\omega)$ is proportional to the corresponding capacitance. In addition to the EFM signals the AFM topography data can be measured. It is worth to note that in NC mode of EFM the oscillations of the probe are almost free, but in DC mode the cantilever is fixed at both ends. In the last case the amplitude of $H(\omega)$ and $H(2\omega)$ signals is determined not only by the corresponding components of the force $F(\omega)$ and $F(2\omega)$, but also by the mechanical hardness

k_{eff} of the probe-surface contact [5]. Due to dependence of k_{eff} on the surface curvature, the DC EFM signals may be mixed with the topographic effect. A straightforward way to suppress this mixing is to study atomically flat surfaces, what requires a careful preparation of the laser heterostructure cleavage.

We have performed measurements in DC mode on the P4-SPM (NT-MDT) microscope and in NC mode on the AFM system Autoprobe CP Research (ThermoMicroscopes). The ac bias is applied to the probe tip made from heavily doped Si at a typical frequency of around 50KHz (300KHz) and a voltage amplitude of 1V (3V), correspondingly in NC (DC) modes of EFM. The NC EFM signals are analyzed through a Stanford Lock-in Amplifier 8230, the lock-in amplifier built in the resonant module of P4-SPM is used for the DC EFM signals detection. The studied lasers are biased by the constant voltage source built in the microscopes.

Figure 1 shows typical sets of the AFM/EFM data used in our work obtained on the cleaved surfaces of two p-i-n laser diodes. The left set of data characterizes the first laser and was measured in DC mode (images a-d); the second laser (the right set of data) was probed in NC mode (images a*-d*). The structures are similar and consist of an n-doped GaAs substrate (**S**), an n-doped (Si) 2 μ m-thick AlGaAs emitter (**N**), an undoped 0.4 μ m-thick GaAs i-waveguide (**W**) centered with 9nm strained quantum well (**QW**), a p-doped (Be) 2 μ m-thick AlGaAs emitter (**P**) followed by heavily doped p-GaAs contact layer (**P⁺**). The topography data images of both structures reveal all the main layers the lasers consist of. The darker contrast corresponds to the depression of the surface relief. The waveguide regions of the structures are several angstroms lower then n- and p- emitters due to known difference in oxide layer thickness on GaAs and AlGaAs [7]. The bright line in the middle of the waveguide corresponds to the compressed InGaNAs (left image) and InGaAs (right image) QWs. As it was shown earlier, thin compressed layers can noticeably extrude out on the cleavage [8]. The DC mode topography image (Figure 1a) has better spatial resolution, than the NC mode topography image (Figure 1a*). From the profile below the Figure 1a one can evaluate approximately 1 angstrom elevation of the QW over the cleavage. Some smearing of the atomic scale variations in the cleavage relief in NC mode topography data seems to be due to the influence of the contamination layer covering the surface in air. In DC mode the probe tip can penetrate through this soft layer, and it does not prevent to map the fine features of the relief.

In Figure 1 b-d (DC mode) and b*-d* (NC mode) the variations of the EFM signals over the studied surface areas are presented. The data were measured at the negative dc bias applied to the n-contact of the lasers, when n-p junctions were almost open. The $H(\omega)$ signal

(potential) images and corresponding profiles in Figures 1b,b* taken in different modes of EFM are almost identical to each other. In both cases the signal has the shape of the double step, with the central plateau corresponding well to the waveguide regions. The visual changes of the $H(\omega)$ signal take place at the interfaces of the waveguides with the n- and p-emitter layers, what means that the main drop of the applied voltage occurs there. It is convenient also to analyze the $\Delta H(\omega)/\Delta x$ data that are calculated numerically along the direction x perpendicular to the interfaces. The meaning of the $\Delta H(\omega)/\Delta x$ data is the electric field magnitude at the surface in the direction perpendicular to the interfaces. Figures 1c,c* show the images and profiles of $\Delta H(\omega)/\Delta x$. The distributions of the electric field have two spikes whose extrema are localized near the waveguide interfaces, while at the waveguide centers the electric field is significantly decreased. The contributions of the spikes at the n-emitter/i-waveguide and i-waveguide/p-emitter interfaces into the inner electric field redistribution under the applied voltage will be considered below. Good correspondence between the measurements in DC and NC modes is also seen in the variations of the $H(2\omega)$ signal (capacitance). The $H(2\omega)$ signal images and profiles are shown in Figure 1d,d*. The white bands in the right (left) part of the image in Figure 1d (1d*) is attributed to the p+-GaAs contact layer (n-GaAs substrate), see also the corresponding topography images in Figure 1a (1a*). An increase of the capacitance at the GaAs compared to the AlGaAs emitters is related to the thinner native oxide on GaAs [7]. The capacitance at the substrate, the emitter layers and p+ contact layer does not depend on the applied bias. However, the applied bias affects strongly the capacitance at the waveguide region, see the wide $\sim 0.4 \mu\text{m}$ plateau in capacitance signal that coincides with the position of the waveguide. For the laser structure studied by DC EFM (Figure 1d), the additional peak in the $H(2\omega)$ signal is observed at the position of the QW. It may be caused by the contribution of the topographic effect in the capacitance signal [5]. In the topography image (Figure 1a) the QW is revealed as small elevation of the relief. Similar coupling between topography and capacitance is responsible for an enhanced contrast of the waveguide interfaces in $H(2\omega)$ image (Figure 1d), since in the topography image (Figure 1a) the waveguide interfaces correspond to the borders of the depression in the relief.

The comparison of the DC and NC modes of EFM can be summarized as follows. In this study only inessential differences in facilities of both EFM modes have been found. Under the atmospheric conditions, the atomic scale variations of the surface relief can be better resolved in DC mode, that is less sensitive to the surface contamination layer. From

the other side, similar signal to noise ratio of the EFM signals is obtained at lower ac amplitudes of excitation (0.5-1 V) in NC mode, than in DC mode (~ 3 V).

To analyze the inner electric field and the capacitance distribution in the AlGaAs/GaAs based laser, we present in Figure 2 the profiles of $\Delta H(\omega)/\Delta x$ and $H(2\omega)$ signals taken under different applied bias. It was already mentioned that the $\Delta H(\omega)/\Delta x$ data (Figure 2a) are related with the electric field at the surface in the direction perpendicular to the interfaces. Variations of this field should reflect variations of the inner electrical field in laser diodes in the same direction. Without bias (a profile taken at -0.05 V) the distribution of the electric field is symmetric and formed by two spikes whose extrema are localized near the waveguide interfaces. For the low level of injection current, the inner electric field is concentrated at the n-emitter/i-waveguide interface (the left spike in the profiles taken at 0.25 V, -0.35 V and -0.75 V is mainly changed). However, under the high level of injection, the redistribution of the inner electric field in favor of the i-waveguide/p-emitter interface is observed (the right spike in the profile taken at -1.05 V is deeper than the left one).

The profiles of the $H(2\omega)$ signal (capacitance) are shown in Figure 2b. The applied bias affects strongly the capacitance at the waveguide region. For the backward biases, the signal has low magnitude. Under the forward bias of approximately -0.35 V, there appears at the middle of the waveguide the spike in the $H(2\omega)$ signal, which amplitude is higher than the signal level at the surrounding emitters. The spike grows in height and broadens with increasing forward bias, and at -1.05 V its top has a shape of a wide ~ 0.4 μ m plateau that coincides well with the position of the waveguide. It is interesting to stress the graduate increase in the level of the $H(2\omega)$ signal at the waveguide region with the transition from the low level to the high level of injection. We believe that this effect is related to the carriers injection into the waveguide and can be used to study the injected carriers distribution.

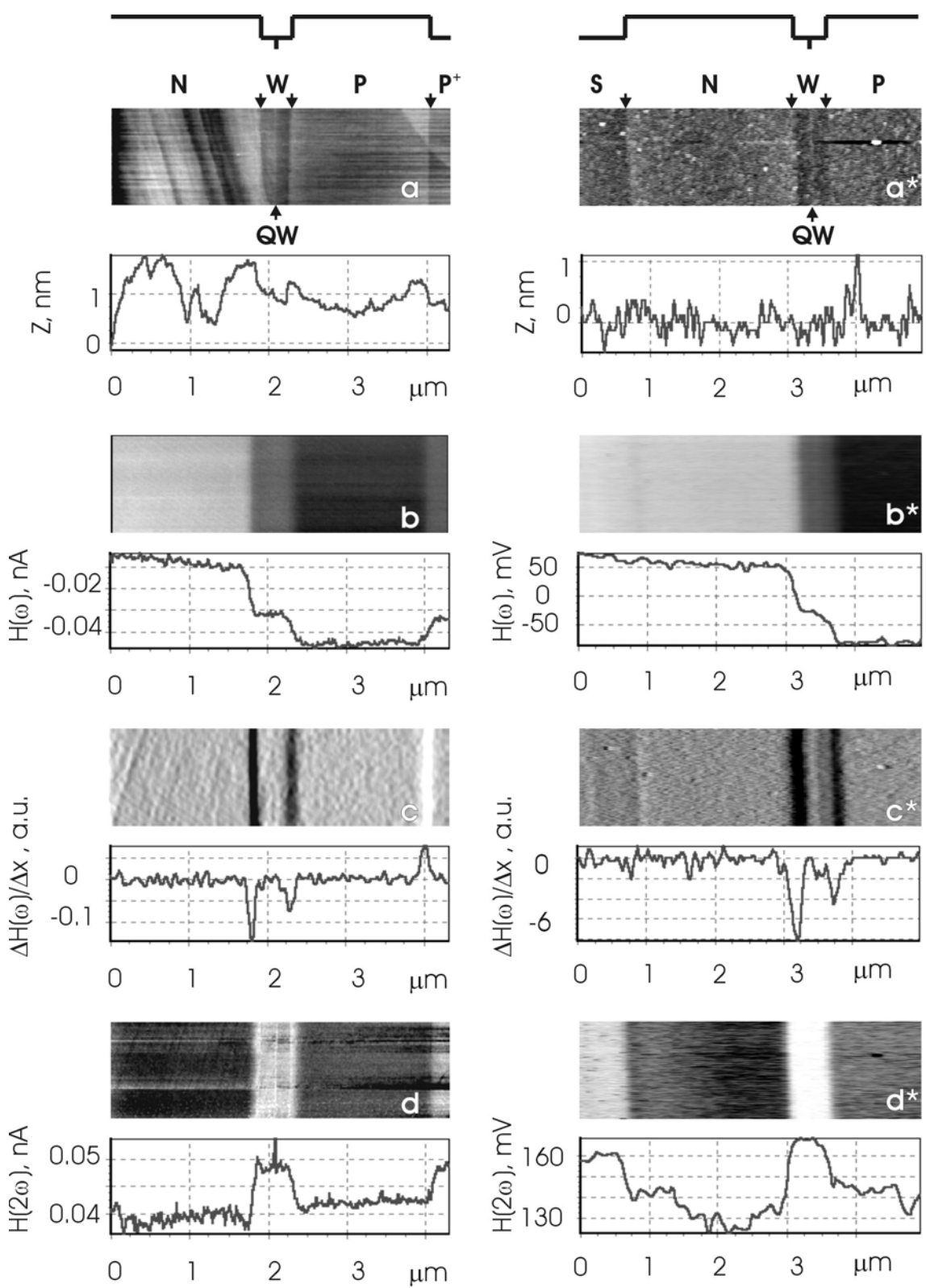
In conclusion, using EFM method we have revealed the fine structures of the inner electric field in AlGaAs/GaAs based p-i-n lasers. It consists of the two spikes at the waveguide/emitters interface, whose relative contribution can be different for forward and backward biases. We have found a strong increase in the capacitance of the waveguide surface area in forward biased laser, that can be related to the level of the injected current. We have also performed a comparison of the DC and NC modes of EFM, and showed that at the atomically flat surface of the laser heterostructures both modes give trusted information.

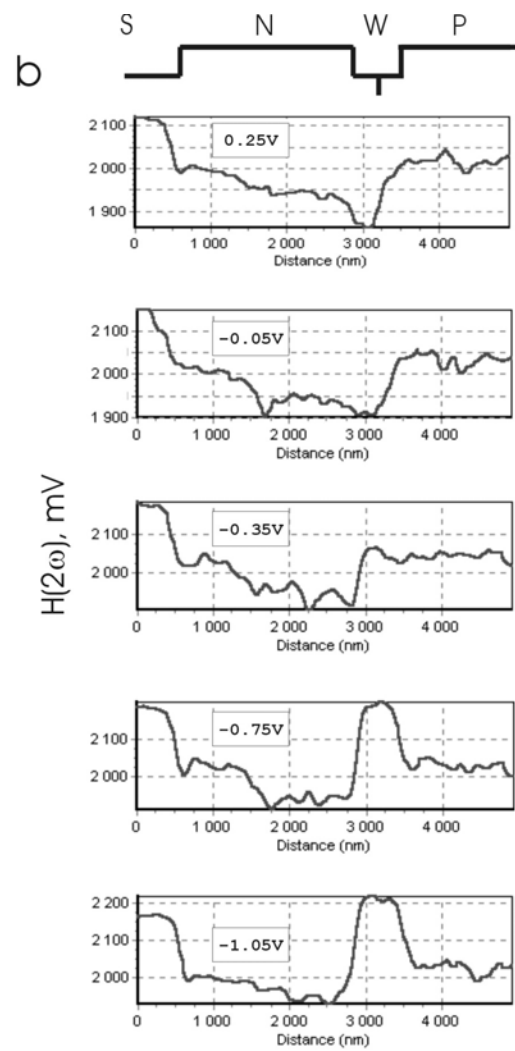
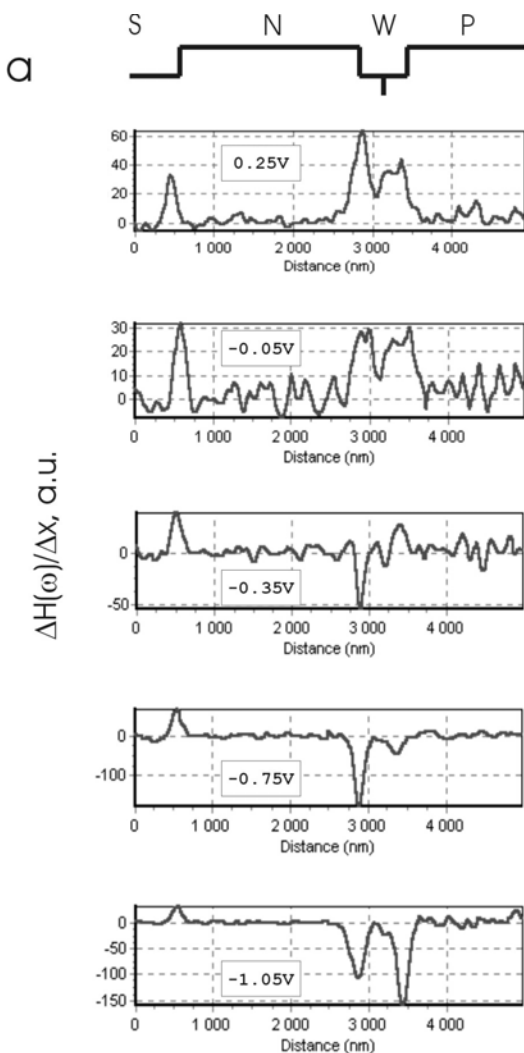
The work was supported by the Program of the Ministry of Science of RF “Physics of Solid State Nanostructures” and by RFBR (grant N 00-02-16948).

Figure captions

Figure 1. The EFM studies in DC and NC (*) modes of two similar laser heterostructures. The images and profiles **a,a*** are the topography data; **b,b*** - the $H(\omega)$ signal (surface potential); **c,c*** - the variations of the $\Delta H(\omega)/\Delta x$ magnitude (electric field); **d,d*** - the $H(2\omega)$ signal (capacitance). The n-p junctions of both lasers are forward biased. The simplified energy band schematics of the lasers are given at the top of the corresponding set of the EFM data.

Figure 2. The dependence of the inner electric field and the capacitance distribution on the applied bias. The $\Delta H(\omega)/\Delta x$ (**a**) and the $H(2\omega)$ (**b**) set of profiles taken at different biases. The dc voltage is applied to the n-contact of the laser structure. The simplified energy band schematics of the laser are given at the top of the corresponding set of the profiles.





References

- [1] M.Nonemacher, M.P.O'Boyle, H.K.Wickramasinghe, *Appl.Phys.Lett.* 58 (1991), 2091
- [2] R.Shikler, T.Meoded, N.Fried, Y.Rosenwaks, *Appl.Phys.Lett.* 74 (1999), 2972
- [3] G.Leveque, P.Girard, E.Skouri, D.Yarekha, *Appl.Surf.Sci.* 157 (2000), 251
- [4] F.Robin, H.Jacobs, O.Homan, A.Stemmer, W.Bächtold, *Appl.Phys.Lett.* 76 (2000), 2907
- [5] J.W.Hong, Sang-il Park, Z.G.Khim, *Rev.Sci.Instr.* 70 (1999), 1735
- [6] A.V.Ankudinov, E.Y.Kotelnikov, A.A.Kanzelson, V.P.Evtikhiev, A.N.Titkov, *Semiconductors* 35, in press (2001)
- [7] A.V.Ankudinov, V.P.Evtikhiev, V.E.Tokranov, V.P.Ulin, A.N.Titkov, *Semiconductors* 33 (1999), 555
- [8] A.V.Ankudinov, A.N.Titkov, T.V.Shubina, S.V.Ivanov, P.S.Kop'ev, H.-J.Lugauer, G.Reuscher, M.Keim, A.Waag, G.Landwehr, *Appl.Phys.Lett.* 75 (1999), 2626